Journal of Experimental Nanoscience

Synthesis and self-assembly of gold nanoparticles using gemini surfactant as a phase transfer reagent and a stabilizer

Jian Xu[a]; Lihui Zhou[a]; Honglai Liu[a]; Ying Hu[a]

[a] Department of Chemistry and Laboratory for Advanced Materials, East China University of Science and Technology, Shanghai 200237, China

PLEASE SCROLL DOWN FOR ARTICLE

Taylor & Francis
Taylor & Francis Group

Synthesis and self-assembly of gold nanoparticles using gemini surfactant as a phase transfer reagent and a stabilizer

JIAN XU, LIHUI ZHOU, HONGLAI LIU* and YING HU

Department of Chemistry and Laboratory for Advanced Materials,
East China University of Science and Technology, Shanghai 200237, China

Gemini surfactant 1,3-bis(cetyldimethylammonium) propane dibromide (16-3-16) was used as a phase transfer reagent as well as a stabilizer to synthesize gold nanoparticles in toluene/water media. The gold nanoparticles were prepared and their self-assembling properties were characterized by UV–visible absorption spectroscopy, infrared spectroscopy and transmission electron microscopy. The results reveal that the 16-3-16 molecules on the surface of gold nanoparticles are in the disordered liquid state. The interparticle spacing can be controlled either physically by the inherent particle-to-particle interactions or chemically by molecular linker.

1. Introduction

Metal nanoparticles are of great interest because their unique properties lead to the appearance of new functions that are notably different from those of the corresponding bulk material [1]. It is widely accepted that metal nanoparticles could serve as fundamental building blocks for future nanotechnology. Size, shape, and surface morphology play pivotal roles in controlling the physical, chemical, optical and electronic properties of these nanomaterials. The phase transfer approach was first used by Brust *et al.* [2] to prepare thiol-stabilized gold nanoparticles. Its application has since been extended to the preparation of metal nanoparticles in recent years [3–8]. For example, Yang *et al.* [4] reported an alternative phase transfer procedure for preparing alkylamine-stabilized Pt nanoparticles. Mayya *et al.* [5] demonstrated the complete transfer from an aqueous to an organic solution of negatively charged carboxylate- and sulfonate-modified gold nanoparticles in the presence of primary amines. Cheng *et al.* [6] presented a method to synthesize gold nanoparticles in a two-phase system by using cetyltrimethylammonium bromide (CTAB) as a phase transfer catalyst.

---

*Corresponding author. Email: hlliu@ecust.edu.cn

Recently, more attention has been paid to the assembly of nanoparticles into well-defined two- and three-dimensional (2D and 3D) superlattices because of their novel properties and potential applications in optical gratings, optical filters, data storage, and microelectronic devices [9–11]. The development of a general method for the fabrication of quantum crystals is a major challenge for future research. Several approaches, such as self-assembly [12–15], Langmuir–Blodgett (LB) techniques [16], and electrophoretic deposition methods [17, 18] have been used to obtain 2D and 3D structures. The basic requirement to initiate ordered self-assembly is to develop stable colloids containing monodisperse nanoparticles with a controlled size and morphology. It is now established that monodisperse lyophobic nanocrystals readily self-assemble into ordered hexagonal close-packed arrays upon solvent evaporation [19]. Following these strategies, many 2D and 3D superstructures of metal nanoparticles [12–18, 20] have been produced.

In this work, gold nanoparticles have been synthesized in a two-phase toluene/water medium using 1,3-bis(cetyldimethylammonium) propane dibromide (16-3-16) as a phase transfer reagent as well as a stabilizer. IR spectra of the 16-3-16 stabilized nanoparticles demonstrated that the alkyl chains in the surface-bound 16-3-16 monolayer are in the disordered liquid state different from the alkanethiol monolayer in the solid state. The 16-3-16 stabilized gold nanoparticles tend to form spontaneously into 2D or 3D structures upon toluene evaporation. The more close-packed particle aggregates can be fabricated by addition of a 1,6-hexanedithiol molecular linker.

2. Experimental

2.1. *Materials*

Tetrachloroauric acid tetrahydrate ($HAuCl_4 \cdot 4H_2O$), toluene, sodium borohydride ($NaBH_4$) and 1,6-hexanedithiol were used without further purification. 1,3-bis(cetyldimethylammonium) propane dibromide (16-3-16) was synthesized according to the literature [21] and recrystallized in ethanol–ethyl acetate mixtures. Deionized water further purified by distillation was used.

2.2. *Synthesis of 16-3-16 stabilized gold nanoparticles*

16-3-16 stabilized gold nanoparticles were synthesized in a two-phase toluene/water medium using $NaBH_4$ as reducing agent. Typically, 40 mL of saturated 16-3-16 toluene solution was mixed with 15 mL of 0.05 mol/L aqueous solution of $HAuCl_4$ under vigorous stirring. Then, the yellow toluene phase was separated, and freshly prepared aqueous $NaBH_4$ solution was added dropwise into the stirred toluene solution until the organic phase changed to dark red indicating the oxidation–reduction reaction occurred with the formation of gold nanoparticles.

2.3. *Characterization*

The UV–vis absorption spectra were obtained on a Shimadzu UV-2450 spectrophotometer. Transmission infrared spectra were collected on a Nicolet Magna-IR 550

spectrometer in the transmission mode. The samples for IR were prepared by casting gold colloid in toluene or 16-3-16 toluene solution onto the transparent KBr disk and dried for 10 min under an infrared lamp. The TEM micrographs were obtained using a JEOL JEM-100CX II electron microscope operating at 100 kV. The samples for TEM were prepared by placing a few drops of gold colloid on to the standard carbon-coated copper grids.

3. Results and discussion

3.1. *Synthesis and characterization of 16-3-16 stabilized gold nanoparticles*

Tetraoctylammonium bromide (TOAB) was usually used as a phase transfer reagent of $HAuCl_4$ from aqueous solution to non-aqueous solution for preparation of gold nanoparticles in a two-phase liquid/liquid system [22]. Similarly, it was found here that gemini surfactant 16-3-16 could also serve successfully as a phase transfer reagent of $HAuCl_4$ from water into toluene. Although the gold salts are solvophobic with respect to toluene, they can be transferred into toluene by complexation with 16-3-16 cations. This process is usually called ion-pair extraction interpreted by solvophobic theory [23]. The extracted gold salts are incorporated into 16-3-16 inverse micelles in toluene, which can be further reduced to gold nanoparticles.

Figure 1 shows the UV–vis absorption spectrum of gold nanoparticles in toluene. A maximum absorption peak at approximately 532 nm originates from the surface plasmon absorption of nanosized gold particles [24].

The FT-IR spectrum of 16-3-16 stabilized gold nanoparticles was collected over the range of 400–3500 cm^{-1} in the transmission mode, as shown in figure 2A. The spectrum is similar to that of the pure 16-3-16 molecules, but some differences are found
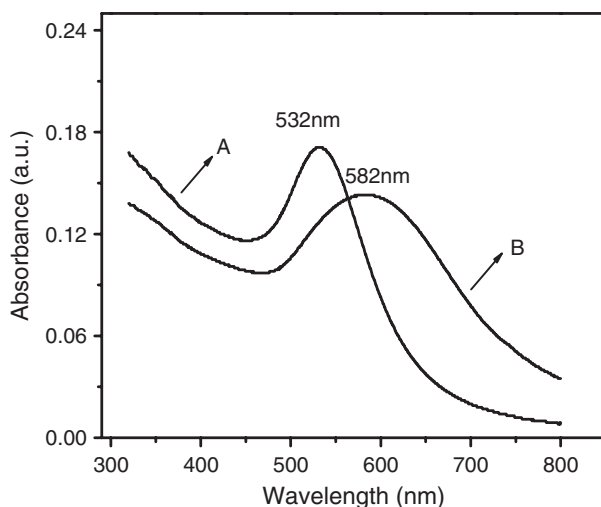

Figure 1. UV–vis absorption spectra of 16-3-16 stabilized gold nanoparticles (A) and 1,6-hexanedithiol linked network (B).
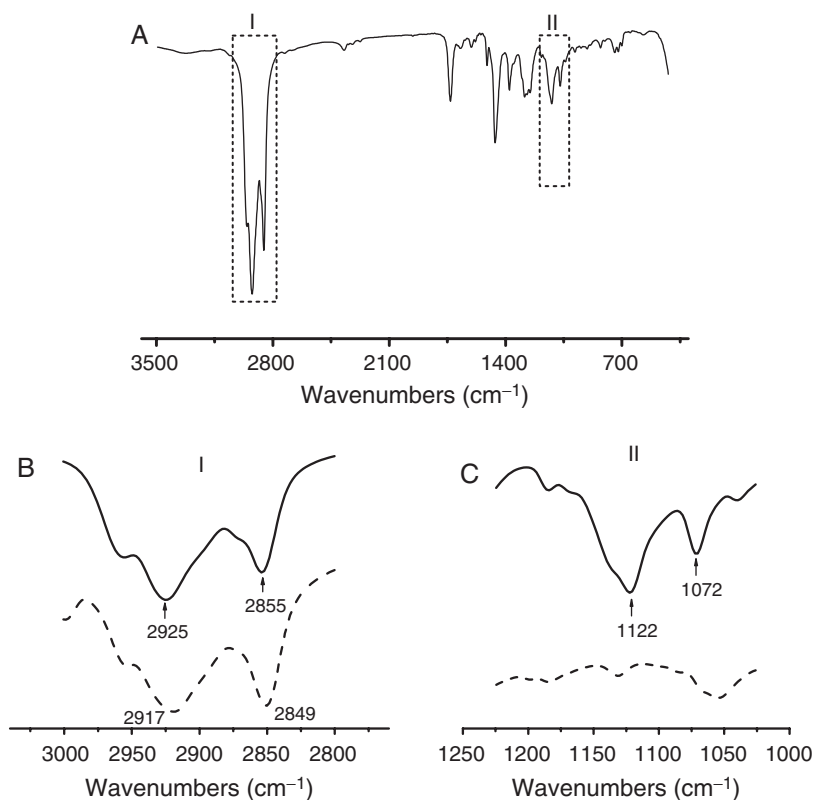
Figure 2. IR spectra of the 16-3-16 stabilized gold nanoparticles (A) and comparison with free 16-3-16 molecules in region I (B) and II (C). (Dash lines are from pure 16-3-16 molecules.)

in the C–H stretching region (I) and the C–C stretching region (II). It is known that the symmetric and antisymmetric CH_2 stretching vibrations can be used as a sensitive indicator of the ordering of the alkyl chains; the higher energies for the CH_2 stretching vibrations indicate greater incidence of *gauche* defects [22, 25]. Figure 2B shows the comparison between free 16-3-16 and 16-3-16 stabilized gold nanoparticles in the C–H stretching vibration region. The symmetric and antisymmetric CH_2 stretching vibrations of pure 16-3-16 lie at 2849 and 2917 cm^{-1}, respectively, whereas the corresponding vibrations of the 16-3-16 stabilized gold nanoparticles appear at 2855 and 2925 cm^{-1}. The energetic shift of CH_2 stretching vibrations indicates a higher density of *gauche* defects in the 16-3-16 stabilized gold nanoparticles than in the pure 16-3-16 molecules. Another change of the spectra is observed in the C–C stretching vibration region (figure 2C). In contrast to the pure 16-3-16 molecules, both the RT (*trans* C–C bonds) and RG (*gauche* C–C bonds) modes are clearly observed in two broad regions centred at 1122 and 1072 cm^{-1}, respectively for the 16-3-16 stabilized gold nanoparticles. The absence of RT and RG modes for pure 16-3-16 molecules indicates that pure 16-3-16 might be in the crystalline state on the KBr disk upon solvent evaporation [6]. The presence of *gauche* C–C stretching vibration in the spectra
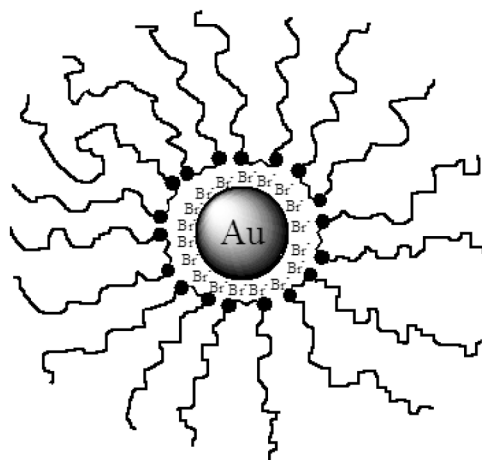
Figure 3.   Schematic illustration of 16-3-16 stabilized gold nanoparticle structure.

of the 16-3-16 stabilized gold nanoparticles is indicative of either a near-surface defect or an internal kink in the 16-3-16 capping layer. The above FT-IR spectral studies of C–H and C–C vibrations show clearly that a higher density of *gauche* defects is induced when 16-3-16 molecules are linked to a gold nanoparticle. Murray and co-workers found that alkanethiolates with comparable chain length are in a solid state, predominantly in the all-*trans* zigzag conformation [22]. It is therefore reasonable to suggest that these 16-3-16 molecules adsorbed on the gold nanoparticle might be in a disordered liquid or glass state [22, 25] different from that of the solid or crystalline state. The higher disorder of 16-3-16 monolayers compared to alkanethiol monolayers [26] with comparable chain length might originate from a larger volume of the ammonium head ($\sim$0.050 nm^3) occupying a larger surface area than the mercapto head ($\sim$0.0044 nm^3). As a result, a larger freedom of movement of the alkane chain would be expected for 16-3-16 monolayers on gold cluster. Based on the above spectral studies, a possible structure of 16-3-16 stabilized gold nanoparticles is illustrated in figure 3. 16-3-16 molecules adsorbed on the gold nanoparticle might form surface ion pairs with Br$^-$ ions attached to the Au surfaces and the cationic 16-3-16 headgroups surround the Br$^-$ layer by electrostatic interactions. The hydrophobic 16-3-16 tail chains would point outward, stabilizing the gold nanoparticles in toluene.

3.2. *Self-assembly of the 16-3-16 stabilized gold nanoparticles*

Similar to the alkanethiol-capped gold nanoparticles [26], the 16-3-16 stabilized gold nanoparticles can organize spontaneously into a 3D or 2D array upon solvent evaporation. Figure 4 shows the TEM micrographs of 3D and 2D particle arrays on a carbon-coated copper grid and particle size distribution of the 16-3-16 stabilized gold nanoparticles. The size distribution of gold nanoparticles is relatively narrow and the average diameter is approximately 7.1 nm. The particles are not arrayed in an orderly manner, which might be due to the relatively low monodispersity of 16-3-16
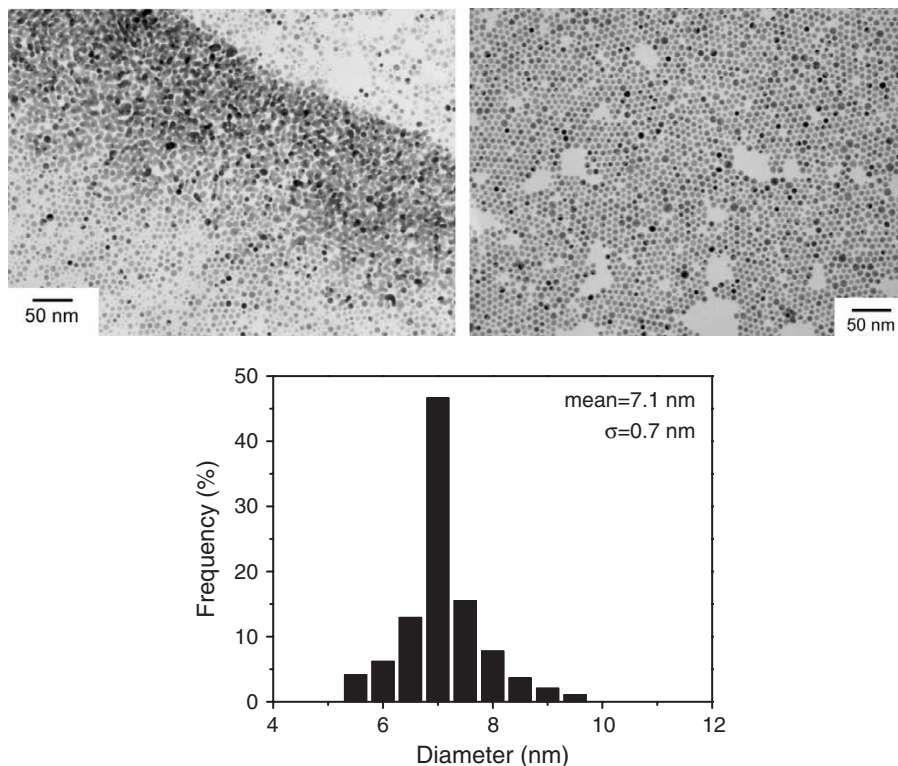
Figure 4.   Typical TEM micrographs and size distribution of the 16-3-16 stabilized gold nanoparticles.

stabilized gold nanoparticles. The average particle-to-particle distance is ∼2 nm smaller than double the length of the 16-3-16 molecule, indicating intertwining of alkyl chains between two adjacent gold nanoparticles similar to the previous studies [27]. In addition, the particles in this array are still discrete and not fused into larger particles showing that gemini surfactant 16-3-16 can stabilize the gold nanoparticles well in this system.

Dithiol has been demonstrated to be a strong ligand, which could link gold nanoparticles into networks [28]. It was found that the colour of the solution changed from red to blue when a small amount of 1,6-hexanedithiol was added into the solution. A red-shift and widening of the maximum absorbance peak were observed as shown in figure 1 (curve B) indicating the chemical aggregation of the gold nanoparticles [29]. Figure 5 shows the TEM micrograph of a 1,6-hexanedithiol linked network of gold nanoparticles and no fused particle is observed. The average particle-to-particle distance is estimated to be ∼1 nm, consistent with the length of 1,6-hexane-dithiol. The distance between the particles is determined by the length of the linker molecule [30].

It is worth mentioning that although particle aggregations are observed on the copper grid for both the as-prepared gold colloid (case I) and the colloid with
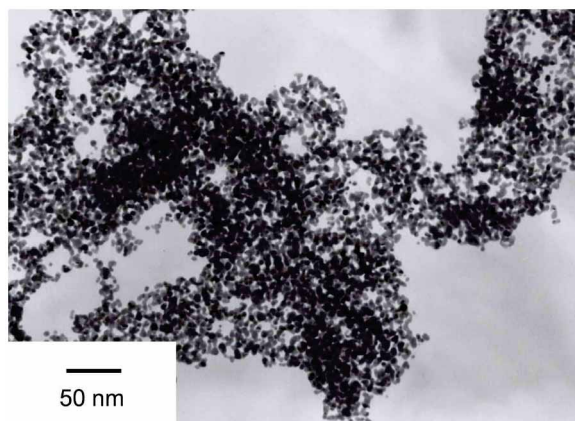
Figure 5. Typical TEM micrograph of 1,6-hexanedithiol linked networks.

dithiol addition (case II), the mechanisms of self-assembling processes are different. Because 16-3-16 stabilized gold nanoparticles are solvophilic with respect to toluene, it is energetically favourable for them to keep their solvation shells to prevent particle aggregation in toluene. In case I, with the evaporation of the solvent, the particles on the copper grid assembled together through intermolecular force of the 16-3-16 molecule on the nanoparticle. Meanwhile, the tail chains of the 16-3-16 molecule form a steric hindrance around the nanoparticles and prevent further aggregation. Thus, the aggregation in case I actually happened on the grid surfaces and the final structure of the formed aggregates might depend on the balance between attraction forces among the 16-3-16 molecules attached on the gold nanoparticle and their steric hindrance. As for the aggregation in case II, due to the strong interaction between the mercapto group and gold, dithiol replaced 16-3-16 ligands and linked gold nanoparticles into networks through chemical interaction when dithiol was added in the gold colloid. The aggregation in case II might happen predominantly in toluene solvent and the drying process would not affect the structure of the network [28].

4. Conclusions

In conclusion, gold nanoparticles were successfully synthesized using gemini surfactant as a phase transfer reagent as well as a stabilizer. The result of IR spectra revealed that the structure of 16-3-16 stabilized nanoparticles can be schematized as shown in figure 3 where the 16-3-16 molecules on the surface of gold nanoparticles are in the disordered liquid state. The 2D or 3D self-assemblies were obtained by solvent evaporation or introduction of a molecular linker; their mechanisms were discussed. This work puts forward the application of gemini surfactant as a phase transfer reagent to synthesize nanoparticles.

Acknowledgements

References

[1] G. A. Ozin. Nanochemistry: synthesis in diminishing dimensions. Adv. Mater. **4**, 612 (1992).

[2] M. Brust, M. Walker, D. Bethell, D. J. Schiffrin, and R. Whyman. Synthesis of thiol-derivatized gold nanoparticles in a two-phase liquid–liquid system. J. Chem. Soc., Chem. Commun. 801 (1994).

[3] G. Viau, R. Brayner, L. Poul, N. Chakroune, E. Lacaze, F. Fievet-Vincent, and F. Fievet. Ruthenium nanoparticles: size, shape, and self-assemblies. Chem. Mater. **15**, 486 (2003).

[4] J. Yang, T. C. Deivaraj, H. P. Too, and J. Y. Lee. An alternative phase-transfer method of preparing alkylamine-stabilized platinum nanoparticles. J. Phys. Chem. B **108**, 2181 (2004).

[5] K. S. Mayya and F. Caruso. Phase transfer of surface-modified gold nanoparticles by hydrophobization with alkylamines. Langmuir **19**, 6987 (2003).

[6] W. Cheng, S. Dong, and E. Wang. Synthesis and self-assembly of cetyltrimethylammonium bromide-capped gold nanoparticles. Langmuir **19**, 9434 (2003).

[7] Y. Wang, J. F. Wong, X. Teng, X. Z. Lin, and H. Yang. 'Pulling' nanoparticles into water: phase transfer of oleic acid stabilized monodisperse nanoparticles into aqueous solutions of α-cyclodextrin. Nano Lett. **3**, 1555 (2003).

[8] G. T. Wei, Z. Yang, C. Y. Lee, H. Y. Yang, and C. R. C. Wang. Aqueous-organic phase transfer of gold nanoparticles and gold nanorods using an ionic liquid. J. Am. Chem. Soc. **126**, 5036 (2004).

[9] A. N. Shipway, E. Katz, and I. Willner. Nanoparticle arrays on surfaces for electronic, optical, and sensor applications. Chem. Phys. Chem. **1**, 18 (2000).

[10] A. Kumar and G. M. Whitesides. Patterned condensation figures as optical diffraction gratings. Science **263**, 60 (1994).

[11] O. Wilson, G. J. Wilson, and P. Mulvaney. Laser writing in polarized silver nanorod films. Adv. Mater. **14**, 1000 (2002).

[12] J. E. Martin, J. P. Wilcoxon, J. Odinek, and P. Provencio. Superlattices of platinum and palladium nanoparticles. J. Phys. Chem. B **106**, 971 (2002).

[13] S. He, J. Yao, P. Jiang, D. Shi, H. Zhang, S. Xie, S. Pang, and H. Gao. Formation of silver nanoparticles and self-assembled two-dimensional ordered superlattice. Langmuir **17**, 1571 (2001).

[14] J. E. Martin, J. Odinek, J. P. Wilcoxon, R. A. Anderson, and P. Provencio. Sintering of alkanethiol-capped gold and platinum nanoclusters. J. Phys. Chem. B **107**, 430 (2003).

[15] S. Stoeva, K. L. Klabunde, C. M. Sorensen, and I. Dragieva. Gram-scale synthesis of monodisperse gold colloids by the solvated metal atom dispersion method and digestive ripening and their organization into two- and three-dimensional structures. J. Am. Chem. Soc. **124**, 2305 (2002).

[16] T. Hassenkam, K. Nørgaard, L. Iversen, C. J. Kiely, M. Brust, and T. Bjørnholm. Fabrication of 2d gold nanowires by self-assembly of gold nanoparticles on water surfaces in the presence of surfactants. Adv. Mater. **14**, 1126 (2002).

[17] S. R. Yeh, M. Seul, and B. I. Shraiman. Assembly of ordered colloidal aggregates by electric-field-induced fluid flow. Nature **386**, 57 (1997).

[18] M. Trau, D. A. Saville, and I. A. Aksay. Field-induced layering of colloidal crystals. Science **272**, 706 (1996).

[19] S. A. Harfenist, Z. L. Wang, R. L. Whetten, I. Vezmar, and M. M. Alvarez. Three-dimensional hexagonal close-packed superlattice of passivated Ag nanocrystals. Adv. Mater. **9** 817 (1997).

[20] J. J. Kakkassery, J. P. Abid, M. Carrara, and D. J. Fermin. Electrochemical and optical properties of two dimensional electrostatic assembly of Au nanocrystals. Faraday Discuss **125**, 157 (2004).

[21] R. Zana, M. Benrraou, and R. Rueff. Alkanediyl-α,ω-bis(dimethylalkylammonium bromide) surfactants. 1. Effect of the spacer chain length on the critical micelle concentration and micelle ionization degree. Langmuir **7**, 1072 (1991).

[22] M. J. Hosterler, J. J. Stokes, and R. W. Murray. Infrared spectroscopy of three-dimensional self-assembled monolayers: *N*-alkanethiolate monolayers on gold cluster compounds. Langmuir **12**, 3604 (1996).

[23] K. Miyabe, S. Taguchi, I. Kasahara, and K. Goto. Interpretation by the solvophobic theory on the linear additive representation of the logarithm of ion-pair extraction constant with individual contributions of cation, anion, and organic solvent. J. Phys. Chem. B **104**, 8481 (2000).

[24] S. Link and M. A. El-Sayed. Size and temperature dependence of the plasmon absorption of colloidal gold nanoparticles. J. Phys. Chem. B **103**, 4212 (1999).

[25] R. G. Snyder, M. Maroncelli, H. L. Strauss, and V. M. Hallmark. Temperature and phase behavior of infrared intensities: the poly(methylene) chain. J. Phys. Chem. **90**, 5623 (1986).

[26] B. L. V. Prasad, S. I. Stoeva, C. M. Sorensen, and K. J. Klabunde. Digestive-ripening agents for gold nanoparticles: alternatives to thiols. Chem. Mater. **15**, 935 (2003).

[27] C. P. Collier, R. J. Saykally, J. J. Shiang, S. E. Henrichs, and J. R. Heath. Reversible tuning of silver quantum dot monolayers through the metal–insulator transition. Science **277**, 1978 (1997).

[28] C. R. Mayer, S. Neveu, and V. Cabuil. 3D hybrid nanonetworks from gold-functionalized nanoparticles. Adv. Mater. **14**, 595 (2002).

[29] S. J. Park, A. A. Lazarides, C. A. Mirkin, and R. L. Letsinger. Directed assembly of periodic materials from protein and oligonucleotide-modified nanoparticle building blocks. Angew. Chem. Int. Ed. **40**, 2909 (2001).

[30] J. P. Novak and D. L. Feldheim. Assembly of phenylacetylene-bridged silver and gold nanoparticle arrays. J. Am. Chem. Soc. **122**, 3979 (2000).